

Abnormal Whole Blood Thrombi in Humans with Inherited Platelet Receptor Defects

Francis J. Castellino^{1*}, Zhong Liang¹, Patrick K. Davis¹, Rashna D. Balsara¹, Harsha Musunuru¹, Deborah L. Donahue¹, Denise L. Smith¹, Mayra J. Sandoval-Cooper¹, Victoria A. Ploplis¹, Mark Walsh^{1,2}

1 W. M. Keck Center for Transgene Research, University of Notre Dame, Notre Dame, Indiana, United States of America, **2** Department of Emergency Medicine, Memorial Hospital of South Bend, South Bend, Indiana, United States of America

Abstract

To delineate the critical features of platelets required for formation and stability of thrombi, thromboelastography and platelet aggregation measurements were employed on whole blood of normal patients and of those with Bernard-Soulier Syndrome (BSS) and Glanzmann's Thrombasthenia (GT). We found that separation of platelet activation, as assessed by platelet aggregation, from that needed to form viscoelastic stable whole blood thrombi, occurred. In normal human blood, ristocetin and collagen aggregated platelets, but did not induce strong viscoelastic thrombi. However, ADP, arachidonic acid, thrombin, and protease-activated-receptor-1 and -4 agonists, stimulated both processes. During this study, we identified the genetic basis of a very rare double heterozygous GP1b deficiency in a BSS patient, along with a new homozygous GP1b inactivating mutation in another BSS patient. In BSS whole blood, ADP responsiveness, as measured by thrombus strength, was diminished, while ADP-induced platelet aggregation was normal. Further, the platelets of 3 additional GT patients showed very weak whole blood platelet aggregation toward the above agonists and provided whole blood thrombi of very low viscoelastic strength. These results indicate that measurements of platelet counts and platelet aggregability do not necessarily correlate with generation of stable thrombi, a potentially significant feature in patient clinical outcomes.

Citation: Castellino FJ, Liang Z, Davis PK, Balsara RD, Musunuru H, et al. (2012) Abnormal Whole Blood Thrombi in Humans with Inherited Platelet Receptor Defects. *PLoS ONE* 7(12): e52878. doi:10.1371/journal.pone.0052878

Editor: Kathleen Freson, University of Leuven, Belgium

Received: September 25, 2012; **Accepted:** November 22, 2012; **Published:** December 28, 2012

Copyright: © 2012 Castellino et al. This is an open-access article distributed under the terms of the Creative Commons Attribution License, which permits unrestricted use, distribution, and reproduction in any medium, provided the original author and source are credited.

Funding: This work was supported by a grant from Memorial Hospital of South Bend. The funders had no role in study design, data collection and analysis, decision to publish, or preparation of the manuscript.

Competing Interests: The authors have declared that no competing interests exist.

* E-mail: fcastell@nd.edu

Introduction

An initial step in thrombus formation in the injured vascular endothelium is the adhesion of platelets to exposed subendothelial components, e.g., von Willebrand Factor (vWF), under high rates of shear, via the interaction of the platelet glycoprotein (GP) 1b/V/IX receptor complex with subendothelial vWF [1]. This tethering of platelets then promotes their firmer binding to subendothelial collagen (COL) fibers via platelet receptors, e.g., GPVI [2,3] and integrin α IIb β 1 [4]. During this process, platelets are activated, leading to platelet shape changes, aggregation, release of aggregation agonists, e.g., ADP and Ca^{2+} , from dense granules, and release of other biologically active agents, e.g., growth factors, hemostasis agents, and adhesion proteins, from α -granules [5]. The elevation of intracellular Ca^{2+} results in enzymatic liberation of arachidonic acid (AA) from phospholipids, subsequently forming thromboxane A₂ (TxA₂), which induces platelet activation. Other signaling events occur as a result of agonist-platelet receptor interactions, one example being ADP interactions with its platelet receptor, P₂Y₁₂ [6], which results in activation of the integrin complex, α IIb β 3, the major fibrinogen receptor on platelets [7]. This step promotes platelet aggregation via fibrinogen bridging and thrombus growth.

Discrete steps of platelet activation have been studied in vitro by exogenous activators, e.g., ADP and AA. Additional studies

employing gene-altered mice and patients with specific platelet dysfunctions, e.g., GPIb defects in Bernard Soulier Syndrome (BSS) [8], and α IIb β 3 abnormalities in Glanzmann's Thrombasthenia (GT), have also been employed to establish mechanisms of platelet function. We propose that additional significant advances can be made by employing the critical end-point of whole blood thrombus-based examination of platelet function, in combination with platelet aggregation studies, which would expand knowledge on relationships between the receptor interactions leading to platelet aggregation and stable thrombus formation. We undertook such a study, with the aid of blood from very rare BSS and GT patients. The results of this investigation are reported herein.

Materials and Methods

Blood Collection

This study was designed to be consistent with the US CFR and ICH Guidelines on Good Clinical Practices. Venous human blood was collected by licensed phlebotomists from 10 normal males and females, two female BSS patients (BSS-1 and BSS-2), both heterozygous parents of one of the BSS (BSS-1M and BSS-2F) patients, one male GT (GT-1) patient, 2 female GT patients (GT-2 and GT-3), and the heterozygous mothers of the two female GT patients (GT-2M and GT-3M), none of whom reported interfering medications or recent platelet infusions. Polystyrene vacutainer

tubes, containing either 3.2% sodium citrate (9:1 v:v), 75 U of Na⁺-heparin, or 1.8 mg EDTA/ml, were used. CBCs and metabolic profiles were rapidly obtained on EDTA-treated blood. PT, aPTT, and fibrinogen levels were determined using Diagnostica Stago (Parsippany, NJ) STArt kits and a STArt-8 hematology analyzer. IRB approval was obtained from Memorial Hospital of South Bend (MHSB) and informed consent forms were signed by all control and subject patients in accord with the Declaration of Helsinki.

Blood Smears

Blood smears were fixed on slides with methanol, stained with Volu-Sol (Salt Lake City, UT) Dip Stain, and fixed with Volu-Sol Stain Solution. The washed and air-dried slides were coverslipped with Permount mounting medium (Electron Microscopy Sciences, Hatfield, PA) and examined microscopically. Platelet sizes, measured as the diameter at the longest axis, were acquired from the images. Each image contained 4–10 platelets/field, and 3–10 images/blood smear were obtained.

Sequencing of WBC DNA

Genomic DNA from WBC was used for PCR cloning of the exons. Traditional Sanger sequencing was accomplished using an ABI 3730x1 96-capillary sequencer with a variety of custom designed primers for the complete exon 2 of the GPIIb gene (*GPIIb*), which contains the entire GPIIb protein open reading frame (ORF), for BSS-1 and BSS-2. Similarly, to identify the genetic abnormalities in GT-1, primers were designed to amplify all 30 exons of the gene (*ITGA2B*) encoding the ORF of integrin α IIb (CD41) and all 15 exons of the gene (*ITGB3*) coding for the ORF of integrin β 3 (CD61), along with the intron flanking regions of each exon to insure integrity of splice sites. 4Peaks software (Amsterdam, The Netherlands) was used for viewing and editing sequence trace files with a Mac OSX 10.6.6 system.

Clot Retraction

Control and subject blood samples were separately drawn into vacutainer serum tubes and allowed to stand vertically undisturbed for 30 min. A Nikon digital SLR camera suspended by a tripod, captured a picture of the specimen along the transverse plane looking vertically down the tube.

Flow Cytometric Analysis (FCA)

Staining of platelets. Staining of platelets from platelet rich plasma (PRP) was performed according to the protocol from BD Biosciences with slight modifications. Freshly drawn blood in heparin was centrifuged at 80×g for 20 min and the top PRP layer was gently removed and fixed with 2% paraformaldehyde at room temperature for 10 min. The platelets were treated 2× with wash solution (1% FBS/1X PBS) with centrifugation at 750×g for 10 min. After the final wash, the platelets were resuspended in 6 ml of this same solution. An aliquot of 100 μ l platelets were utilized to label with rabbit-anti-human β 3 antibody (1:10 dilution) (#AP8672b, Abgent, San Diego, CA). This antibody recognizes the peptide region 740–769 at the C-terminal β 3 region of GPIIIa. After 30 min at room temperature, the platelets were washed once and then incubated with donkey-anti-rabbit Alexa Fluor488-conjugated 2° antibody (Molecular Probes, Carlsbad, CA) in the dark for 30 min at room temperature.

Aliquots (100 μ l) of fixed platelets were also labeled for different experiments with 0.125 μ g each of FITC mouse anti-human α IIb antibody (#555466, BD Pharmingen, San Jose, CA), FITC mouse anti-human β 3 antibody (#555753 BD Pharmingen), PE mouse

anti-human GPIIb antibody (#555473 BD Pharmingen), PE mouse anti-human α 2b antibody (integrin β 1) (#556049 BD Pharmingen), FITC mouse anti-human GPIa (integrin α 2) (BD Pharmingen #555498), PE mouse IgG1 isotype control (#555749 BD Pharmingen), and FITC mouse IgG1 isotype control (#555748, BD Pharmingen). All labeled platelet suspensions platelets were finally washed once, resuspended in 1% paraformaldehyde, and analyzed by FCA.

FCA of labeled platelets. A 3 laser 9 color FACSaria III (BD Biosciences, San Jose, CA) was utilized for FCA of the labeled platelets using the FITC and PE channels. Acquisition and analysis were performed by gating on side scatter (SSC-H) and fluorescence (FITC- β 3), setting the scales to logarithmic amplification. Cells in suspension were analyzed at a flow rate of 1 ml/sec and 10,000 events were recorded for analysis.

Thromboelastography (TEG)

For TEG analyses of recalcified whole blood, 20 μ l of 0.2 M CaCl₂ was added to 340 μ l of citrated blood. Data were collected for 1.5–2.0 hr. Rapid thromboelastograms were obtained after addition of 20 μ l of 0.2 M CaCl₂ and 10 μ l of the Rapid TEG kit mixture (Haemoscope, Niles, IL), containing reconstituted soluble human Tissue Factor (sTF)/kaolin/phospholipid, to 340 μ l of citrated blood. Thrombin-enhanced thromboelastograms contained 1 unit thrombin (ERL, South Bend, IN)/20 μ l 0.2 M CaCl₂ and 340 μ l of citrated blood. Kaolin-stimulated thromboelastograms were obtained using 1 ml of citrated whole blood and kaolin solution (Haemoscope). Then, 360 μ l of blood was placed in the cup with 20 μ l of 0.2 M CaCl₂. To assess the competency of the human fibrinolytic system, 200 ng of human tissue-type plasminogen activator (htPA) \pm 5 mM ϵ -aminocaproic acid (EACA), was added to the reaction vessels along with the Ca²⁺/sTF/kaolin sample.

TEG data were collected using an automated Thromboelastograph 5000 (Haemoscope) and analyzed using Haemoscope TAS Version 4.3 Software. The hemostasis parameters obtained were: R, the time from the start of the reaction until the onset of thrombus formation; K₂₀, the time from R to a 20-mm clot strength signal; A, the angle in degrees, which reflects the rate of clot formation; MA_{max}, the maximum amplitude (mm) attained, which is a reflection of the contributions of crosslinked fibrin and platelets to thrombus strength; and the fibrinolysis parameters, LY₃₀ and LY₆₀, which are the percent reductions of the area under the thromboelastograms from the time that MA_{max} is attained until 30 and 60 min, respectively, after MA_{max}.

Platelet Functionality in Thrombus Formation Measured by TEG

For TEG-based platelet analyses, 360 μ l of the kaolin/blood sample was added to 20 μ l of saline/20 μ l of 0.2 M CaCl₂. In a separate reaction cup, 10 μ l of the Activator F kit (reptilase+human (h)FXIIIa) was mixed with 360 μ l of heparinized blood to obtain the contribution to the MA_{max} of crosslinked fibrin alone (MA_F). In other assays, 10 μ l of Activator F and 360 μ l of heparinized blood were employed, and either the recommended 10 μ l of the ADP kit solution, 10 μ l of the AA kit solution, 12 μ l of 10 mg/ml ristocetin (RIST), 10 μ l of 100 μ g/ml of COL; 12 μ l of 1 mM of the protease activated receptor (PAR)-1 agonist, PA-1 (H-SFLLRN-OH; Anaspec, Fremont, CA), or 12 μ l of 20 mM PAR-4 agonist, PA-4 (H-GYPGKF-NH₂; Anaspec), to activate platelets. The MA_{max} for the reaction obtained with each platelet activator - MA_F provides MA_p. The MA_{max} with Ca²⁺/kaolin - MA_F, yields MA_K. The % stimulations were calculated as: MA_p/MA_K×100.

Platelet Aggregometry

For human blood, 300 μ l saline and 300 μ l heparinized blood were mixed in the reaction cup of a Multiplate impedance aggregometer (Verum Diagnostica, Munich, Germany), followed by a 3 min incubation. Then, 20 μ l of 0.2 mM ADP, 20 μ l of 15 mM AA, 20 μ l of 100 μ g/ml COL, 50 μ l of 10 mg/ml RIST, 20 μ l of 1 mM PA-1, or 12 μ l of 20 mM PA-4 were added and recordings initiated.

In all cases, measurements were recorded for 6 min and plotted by the software as arbitrary aggregation units (AU) versus time. The areas under each curve, from 0–6 min, were taken as the platelet aggregation response.

Results

BSS Patients

Two of these extremely rare patients were identified for study and were diagnosed in other facilities earlier in life.

Patient BSS-1. This patient is a 21-year old Caucasian female from a nonconsanguineous parental relationship, diagnosed with BSS at age 7, who has had numerous platelet transfusions throughout her life. At presentation to our facilities, her CBC was normal, except for platelet counts of 28K/ μ l–50K/ μ l on three occasions 2–3 months apart (Table 1). Her blood smears displayed large and giant platelets (Figure 1A–a; Table 1), with 72% $>4 \mu$ m, compared to a normal control (Figure 1A–b; Table 1). Her plasma PT, aPTT, and fibrinogen levels were normal (Table 1), indicating that plasma-based hemostasis was unaffected by her disease.

Patient BSS-2. This patient is a 61-year old Hispanic female diagnosed with BSS at age 2, also frequently administered platelets for clinical procedures, but none within a month of her 3 visits to us that occurred 4 months apart. Her PT, aPTT, and fibrinogen levels were also normal (Table 1). While her WBC count was also normal, her blood sample also showed macrothrombocytopenia (Figure 1A–c; Table 1), with large (4–8 μ m) and giant ($>8 \mu$ m) platelets present, the latter comprising approximately 17% of her total platelets (Table 1).

Whole Clot Retraction of BSS Blood

Whole blood clot retraction studies, an important property of functional platelets, showed a clear clot retraction ring in control normal blood (Figure 1B–a), as well as for the blood of BSS-1 (Figure 1B–b), reflecting the formation of a thrombus that retracts from the sides of the tube. This property of platelets stimulates healthy wound healing, and suggests normal platelet function in this regard. Whole blood clot retraction for BSS-2 blood was also normal (Figure 1B–c).

Molecular Genetics of BSS Patients

Patient BSS-1. Based on our sequence analysis of the *GPIBA* gene of BSS-1, she was determined to be doubly heterozygous for *GPIBA* gene mutations. Of the genomic DNA clones tested, 6 showed deletion of a single nucleotide, G⁹⁵² (numbered from the A¹TG translation initiation site), altering translation to A³¹⁸P (the Met at the translation initiation site is designated amino acid 1), followed by a frame-shift mutation (Figure 2A, B) and a stop codon beginning at sequence position-334. This *GPIBA* mutation has not been previously identified in BSS. After *in silico* reinsertion of G⁹⁵² and translation, the protein showed two tandem exact 13-amino acid residues repeats, at amino acids 415–440, in the VNTR locus of the protein (allele C of GPIb). Variable numbers (1–4) of these polymorphic tandem exact VTNR repeats in GPIb have been reported [9]. Other polymorphisms have been noted in this protein and have assisted in tracking the genetic pools of the

mutations leading to BSS. GPIb, associated with the G⁹⁵² deletion in BSS-1, does not carry the RS polymorphism (T to C) at nucleotide-5 [10], the T¹⁶¹M protein polymorphism (Ko) [11], the silent EF polymorphism (C to T) at the 3rd nucleotide of N²⁵⁸ [10], or the silent KL polymorphism (A to G) at the 3rd nucleotide of R³⁵⁸ [10].

Another group of 9 clones, showed that two nucleotides (A¹⁵⁶²–T¹⁵⁶³) of *GPIBA* were deleted (Figure 2C,D), altering translation to Y⁵²¹C in the transmembrane domain of the protein, followed by a frame-shift mutation, resulting in a stop codon at sequence position 602. This latter mutation has been reported in other BSS patients [12,13]. The translated sequence of the protein, with *in silico* reinsertion of the two deleted nucleotides, showed it also to be allele C in the VNTR locus of GPIb. The gene associated with *GPIBA*[Δ A¹⁵⁶²–T¹⁵⁶³] carries the RS and KL polymorphisms, but not the Ko or EF polymorphisms, in common with the previous two patients described with this altered allele [12,13]. No WT *GPIBA* subclones were found in the DNA of BSS-1.

Blood was obtained from the biological parents of BSS-1 for the study, and both proved to be carriers of one of the two mutations within the *GPIBA* gene of the daughter. Their sequence data were clear in that the paternal *GPIBA* mutant allele possessed *GPIBA*[Δ G⁹⁵²] (11/23 subclones), and its translation after reinsertion of G⁹⁵² showed the protein to contain allele C in GPIb, but no other *GPIBA* polymorphism. The father of BSS-1 also carried WT *GPIBA* 12/23 subclones). The maternal *GPIBA* mutant allele possessed *GPIBA*[Δ A¹⁵⁶²–T¹⁵⁶³] (3/9 subclones), and, after *in silico* reinsertion of A¹⁵⁶²–T¹⁵⁶³ and translation, the protein also contained allele C of *GPIBA*, and the RS and KL polymorphisms. The maternal genomic DNA also possessed WT *GPIBA* (6/9 subclones). The CBCs of each parent were within normal limits, but the paternal manual platelet count was low at 39K/ μ l. Blood smears showed large platelets (34% 4–8 μ m). The maternal platelet count was 174K/ μ l and platelet sizes were normal (95% 2–4 μ m).

Patient BSS-2. Biological relatives of BSS-2 were unavailable. Nonetheless, we suspected the presence of a homozygous double deficiency of *GPIBA*, since her parents were 2nd cousins, as reported by BSS-2. Our sequence analysis of her *GPIBA* gene revealed one population of subclones (20 total), with a deletion of one T in a T-rich segment of the DNA, viz., C⁶¹⁸TTTTTTG in control *GPIBA* and C⁶¹⁸TTTTTTG in the patient sample (Figure 2E,F), a mutation that has not been previously reported in BSS. This change generated a F²⁰⁸L mutation in the patient GPIb, followed by a frame-shift mutation in the gene resulting in a stop codon at sequence position 255. Examination of the remainder of the DNA and translated product, after *in silico* reinsertion of the deleted T, showed it to possess the C allele in the VTNR region of *GPIBA*, but not the RS, Ko, EF, or KL polymorphisms.

We thus conclude that the three allelic mutated *GPIBA* genes that are present in BSS-1 and BSS-2 originated from different founder lines, and BSS-1 represents an extremely rare case of a double heterozygote for two different GPIb inactivating mutations, resulting in BSS. There is no evidence of consanguinity in the family of BSS-1. Thus, this genetic trait resulted from a chance breeding of two different founder lines. To our knowledge, only one other double heterozygote for a GPIb-deficient BSS patient has been fully characterized, and contains separate allelic protein mutations of [C⁸¹R] (renumbered according to our system for consistency) and [W⁵²⁷stop] [14]. These published mutations differ from those described herein. On the other hand, BSS-2 is homozygous for *GPIBA* inactivating mutations, also resulting in

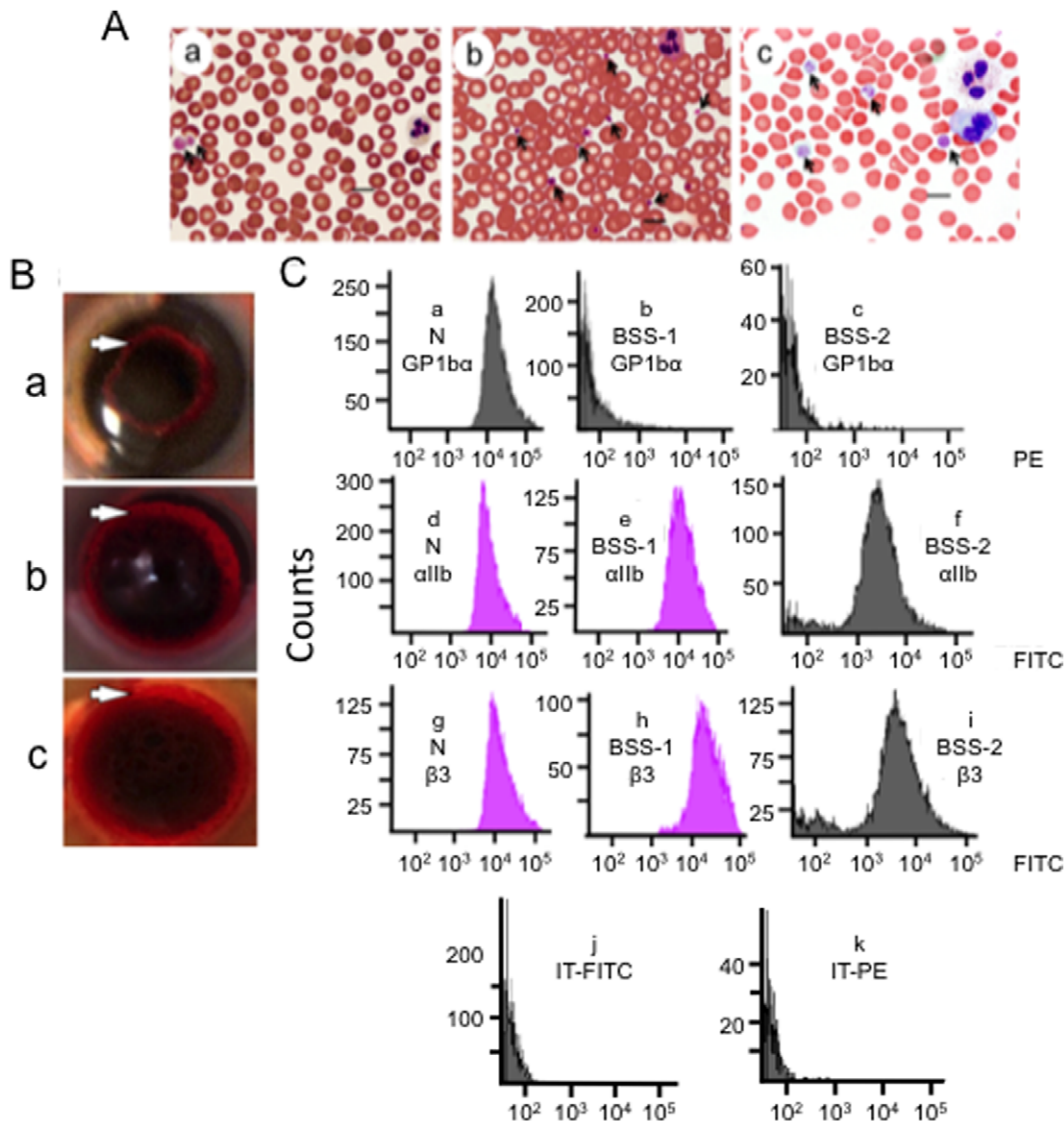


Figure 1. Platelets of BSS patients. (A) Blood smears were stained with Volu-Sol Dip Stain. (a) BSS-1. The platelets (arrows) vary in size and exhibit a granular composition with a fuzzy coat. Giant platelets ($>5 \mu\text{m}$) are indicated by arrows. (b). Normal blood showing platelets (arrows) at $1\text{--}3 \mu\text{m}$ diameter. (c) BSS-2. Giant platelets ($>5 \mu\text{m}$) are indicated by arrows. The blood smears were viewed with a Nikon E600 Eclipse microscope containing a Plan Apo VC $100\times/1.40$ N.A. Oil lens, acquired with a Nikon DS Ri1 color digital camera via Nikon Elements AR 3.2 imaging software, and saved as TIFF files. Measurements of cells were obtained with the measurement tool of the Nikon Elements-AR 3.2 imaging software. The bars on all images represent $10 \mu\text{m}$. (B) Whole blood clot retraction of (a) BSS-1, (b) normal human, and (c) BSS-2 clots. Similar rings of retraction (white arrows) are observed in normal control and BSS blood after 30 min. (C) Flow cytometric analysis of formaldehyde-fixed platelets of PRP from normal (N) blood and PRP from BSS-1 and BSS-2. Surface expression of platelet $\text{GP1b}\alpha$ (CD42b) in (a) normal control. $\text{GP1b}\alpha$ is greatly reduced and similar to the isotype control in (b) BSS-1 and (c) BSS-2 platelets. Surface expression of integrin αIIb (CD41) in a (d) normal control, as well as (e) BSS-1 and (f) BSS-2 platelets. Surface expression of integrin $\beta 3$ (CD41) in $\alpha\text{IIb}/\beta 3$ in a (g) normal control, and (h) BSS-1 and (i) BSS-2 platelets. Normal-to-increased expression of integrin αIIb and the $\alpha\text{IIb}/\beta 3$ complex is observed in BSS platelets. (j, k) Isotype control for (j) FITC and (k) PE with normal platelets; BSS-1, BSS-2, GT-1, GT-2, and GT-3 platelets showed very similar controls. doi:10.1371/journal.pone.0052878.g001

BSS, that originated from a consanguineous breeding of a single founder line, a more common occurrence in BSS.

FCA of BSS Platelets

PRP isolated from a normal control (N) showed the presence of the platelet surface receptors, $\text{GP1b}\alpha$ (Figure 1C-a), integrin αIIb (Figure 1C-d), and integrin $\beta 3$ in $\alpha\text{IIb}/\beta 3$ (Figure 1C-g). On the other hand, PRP from BSS-1 and BSS-2 demonstrated the absence $\text{GP1b}\alpha$ (Figure 1C-b and Figure 1C-c). BSS-1 showed intact-to-increased amounts of integrins αIIb (Figure 1C-e) and $\beta 3$

in $\alpha\text{IIb}/\beta 3$ (Figure 1C-h), and BSS-2 demonstrated near normal levels ($>75\%$) of αIIb (Figure 1C-f) and $\beta 3$ in $\alpha\text{IIb}/\beta 3$ (Figure 1C-i). Thus, the interaction of VWF with platelets is adversely affected by the loss of $\text{GP1b}\alpha$, but contains both protein components of the fibrinogen receptor, $\alpha\text{IIb}/\beta 3$.

GT Patients

Three of these very rare patients were studied.

Patient GT-1. This 61-year old male, diagnosed with GT in the mid-1960s, is the offspring of nonconsanguineous parents.

Table 1. CBC and plasma hemostasis parameters.

Human	Fibrinogen (mg/dl)	PT (sec)	aPTT (sec)	Platelets ^c ($\times 10^3/\mu\text{l}$)	Hemoglobin (g/dl)	WBC ($\times 10^3/\mu\text{l}$)
Controls ^a	272 \pm 13	11.5 \pm 0.2	32.0 \pm 1.1	227 \pm 36 24%, 1–2 μm^{d} 76%, 2–4 μm^{d}	13.9 \pm 0.4	7.1 \pm 0.5
BSS-1 ^b	264; 261	nd; 11.2	33.5; 29.4	37 \pm 7 28%, 1–2 μm^{d} 68%, 2–4 μm^{d} 4%, 4–8 μm^{d}	11.5; 11.7	5.8; 6.7
BSS-2 ^b	384; 317; 351	10.9; 10.5; 10.4	24.9; 26.3; 26.3	59; 32 0; 14%, 1–2 μm^{d} 17; 5%, 2–4 μm^{d} 66; 38%, 4–8 μm^{d} 17; 43%, 8–12 μm^{d}	13.6; 13.6	7.5; 9.3
GT-1 ^b	402; 428; 390	9.9; 10.5; 10.2	24.7; 26.6; 25.6	130; 130; 117 3%, 1–2 μm^{d} 53%, 2–4 μm^{d} 43%, 4–6 μm^{d} 2%, 6–8 μm^{d}	12.8; 13.5; 13.2	3.4; 3.5; 3.7
GT-2	282	10.8	25.6	202 4%, 1–2 μm^{d} 68%, 2–4 μm^{d} 28%, 4–6 μm^{d}	11.2	8.7
GT-3	337	10.2	27.0	224 3%, 1–2 μm^{d} 72%, 2–4 μm^{d} 25%, 4–8 μm^{d}	13.7	7.9

^aNormal human controls, N = 10.

^bData are from separate blood draws >4 months apart.

^cManual counts with Wright stain.

^dAverage size distribution of platelets.

doi:10.1371/journal.pone.0052878.t001

Only patient blood was available, since his parents are deceased and there are no siblings. Plasma-based coagulation assays for GT-1 were found to be within the normal range, although his fibrinogen level was at the high end of normal (Table 1). Platelet counts of GT-1 were at the lower limit of normal and, by manual counts, the size distributions of GT-1 platelets had components (45%) that were larger than normal (Table 1). The hemoglobin concentration of GT-1 was normal, while the WBC count was low (Table 1).

Patient GT-2. This patient is a female offspring of non-consanguineous parents who was diagnosed with GT at 4 weeks of age. She was 20 years of age upon arrival to our facilities, accompanied by her biological mother (GT-2M), who did not show outward symptoms of GT, and did not report a history of the disease. GT-2M provided blood for this study. Plasma-based coagulation assays on GT-2 were found to be normal, as were platelet and WBC counts (Table 1). The size distribution of the platelets of GT-2 were similar to GT-1 and had a small population of large platelets (Table 1).

Patient GT-3. This 16-year old Caucasian female was diagnosed with GT at age 3 years because of frequent and severe nosebleeds. She also has a history of bruising very easily. This patient has had one platelet transfusion because of nosebleeds (age uncertain). At various times, GT-3 has been administered rFVIIa, amicar, and tranexamic acid for nosebleeds. Apparently, she was provided rFVIIa elsewhere for self-administration when needed. She is taking low dose estrogen and reports recent normal menstrual cycles. Plasma coagulation parameters, as well as CBCs, were normal (Table 1) and her cells showed a small population of slightly larger platelets >4 μm . GT-3 was accompanied to our facilities by her asymptomatic mother (GT-3M), who also volunteered blood for this study.

Molecular Genetics of GT Patients

Patient GT-1. Genetic analyses had not been previously performed on patient GT-1. Thus, nucleotide sequences of all exons of the *ITGA2B* (integrin αIIb) and *ITGB3* (integrin $\beta 3$) were determined on this patient. In total, the primers designed provided amplicons covering all exons and splice sites in both genes and

about 50% of the introns. These sequences were compared to those of *ITGA2B* and *ITGB3* in the GenBank database.

We did not find mutations in *ITGA2B* exons. As with WT *ITGA2B*, introns 5 and 8 were flanked by the GC-AG dinucleotide donor and acceptor sequences at their 5' and 3' termini, respectively. The GC-AG splice site is the major (~1%) variant of the standard GT-AG (99%) sequences found at intron flanking positions, and is recognized by the spliceosome [15]. Thus, *ITGA2B* appears genetically intact in this patient. The *ITGB3* gene showed two high frequency mutations in its exons in the patient samples. In one, a [$\text{G}^{30,612}\text{C}$] alteration (Figure 3A, B) occurred (numbered from the A¹TG translation initiation site) located in exon 4, which is the 2nd nucleotide of the DNA codon (CGG) for R¹³¹ in WT- $\beta 3$ integrin (the Met at the translation initiation site is amino acid 1). This mutation yields the DNA codon, CCG, translating to P¹³¹, thus providing the mutated protein, integrin $\beta 3[\text{R}^{131}\text{P}]$. This same change occurred in 6/11 subclones sequenced, suggesting that this mutation is present on one allele of the patient. A total of 5/11 subclones showed the WT codon for amino acid R¹³¹ at this location, thus demonstrating that the $\beta 3$ is heterozygous for the [R^{131}P] mutation, which likely occurred from one parent. All introns were flanked by the standard consensus dinucleotide sequences, GT-AG, at the 5' and 3' termini of the introns, respectively, in at least 8/8 subclones sequenced.

A second mutation was found in another location of the *ITGB3* gene of GT-1, specifically insertion of an A^{38,427} (Figure 3C, D), located in exon 10. This mutation altered the WT-AAT codon to AAA, providing the mutation, [N^{470}K], and altering the reading frame such that a [$\text{S}^{471}\text{stop}$] occurred in the $\beta 3$ protein. A total of 5/11 subclones contained this mutation, while the others displayed the WT amino acid, S⁴⁷¹, at this position. This mutation most likely occurred in the other parental allele. No other alterations occurred in the exons or intron splice junctions in *ITGB3* in this patient.

Thus, the complete genetic data show that GT-1 is doubly heterozygous in the *ITGB3* alleles, with one parent providing the [R^{131}P] mutation, and the other transmitting the [$\text{N}^{470}\text{S}^{471}$]/[$\text{K}^{471}\text{stop}$] mutations. Since GT is an autosomal recessive disorder, it would appear that either mutation, in itself, would inactivate the $\alpha\text{IIb}/\beta 3$ complex, thus severely attenuating fibrin(ogen)-dependent platelet aggregation and platelet contribu-

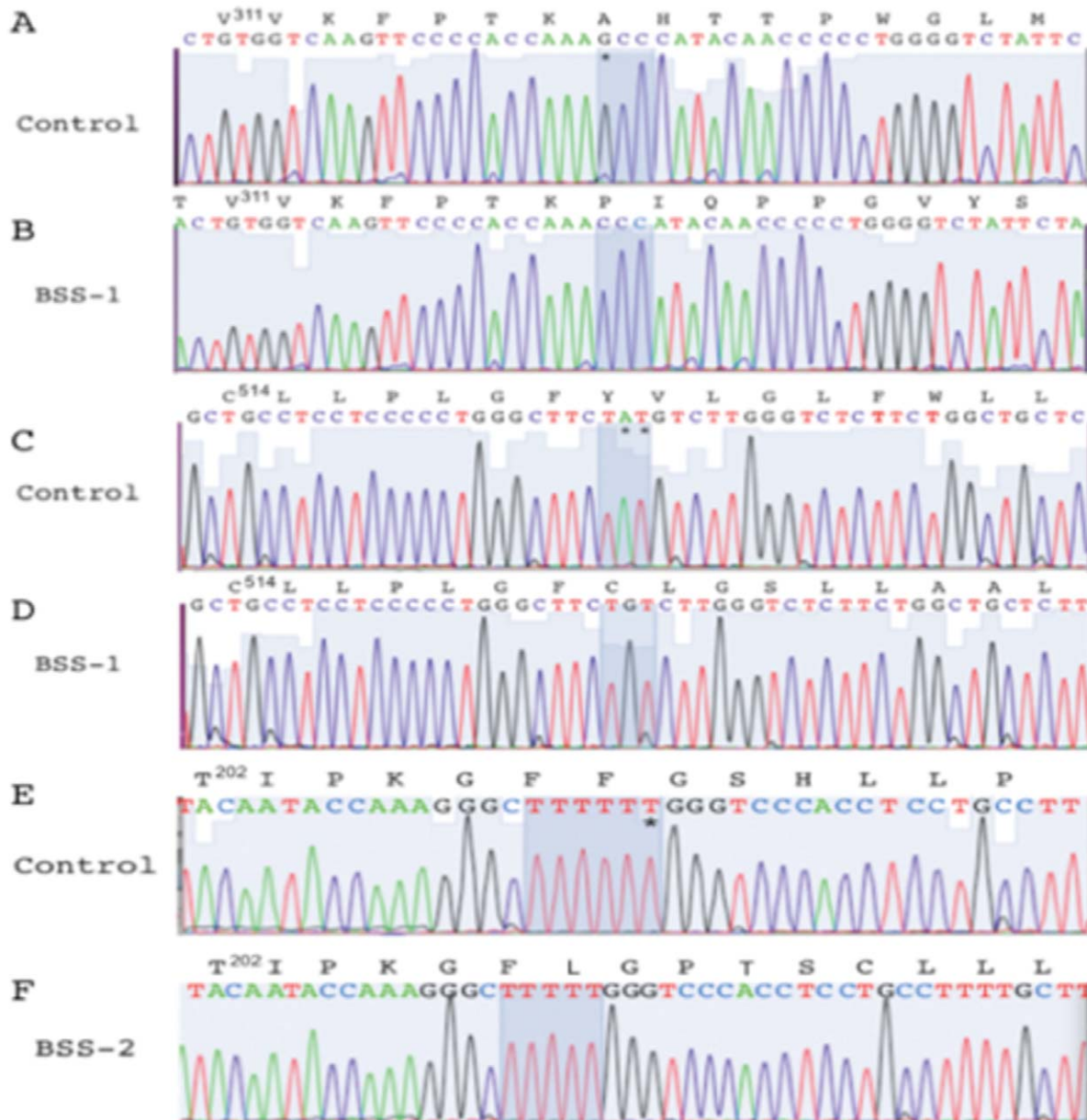


Figure 2. Nucleotide sequence of the mutated regions of *GPIBA* in BSS patients. In each case, the sequence data are displayed for one example PCR clone within the *GPIBA* gene in the genome, along with the readouts of the nucleotides of the translated products. No uncertainties were noted in any clones sequenced in these regions. (A) Normal human *GPIBA* sequence of the region spanning amino acids V³¹¹–M³²⁶ of GP1b. (B) The 1st nucleotide (G*) of the codon for A³¹⁸ is deleted in the paternal allele of BSS-1 (A), thus altering the reading frame of the protein. (C) Normal human GP1b sequence of the region spanning amino acids C⁵¹⁴–L⁵²⁹. (D) The 2nd and 3rd nucleotides (A*T*) of the codon for V⁵²¹ are deleted in the maternal allele of BSS-1 (C), thus altering the reading frame of the protein. (E) Normal human GP1b sequence of the region spanning amino acids T²⁰²–V²¹⁴. (F) A single T of the group of 6 T residues encoding F²⁰⁷–F²⁰⁸ of GP1b has been deleted (*) in both alleles of BSS-2 (E), altering the reading frame of the protein. The protein sequences are numbered from M1 of the ORF. The corresponding nucleotide sequences are numbered from the 1st residue of the ATG translation initiation sequence.
doi:10.1371/journal.pone.0052878.g002

tions to stable clot formation, as is seen experimentally. We conclude that patient GT-1 is a double heterozygote of two $\beta 3$ integrin inactivating mutations.

Patient GT-2. The genetics of GT-2 have been previously studied and a 6 residue deletion (G¹³⁹²TAGAC; numbered from A¹TG) was found in exon 13 of the *ITG2AB* gene [16], corresponding to a 2 amino acid (V⁴⁵³D⁴⁵⁴; numbered from M¹) deletion in integrin α Ib protein. This deletion eliminated two highly conserved amino acids from the fourth Ca²⁺ binding

domain of α Ib, resulting in diminished surface expression of α Ib and a loss of the native conformation of the heterodimeric α Ib/ $\beta 3$.

Patient GT-3. Molecular genetic testing was not performed on GT-3 or GT-3M.

Deposition of Nucleotide Sequences

Nucleotide sequences of the abnormal maternal (BSS-1M) and paternal (BSS-1F) *GPIBA* alleles, both of which are inherited by

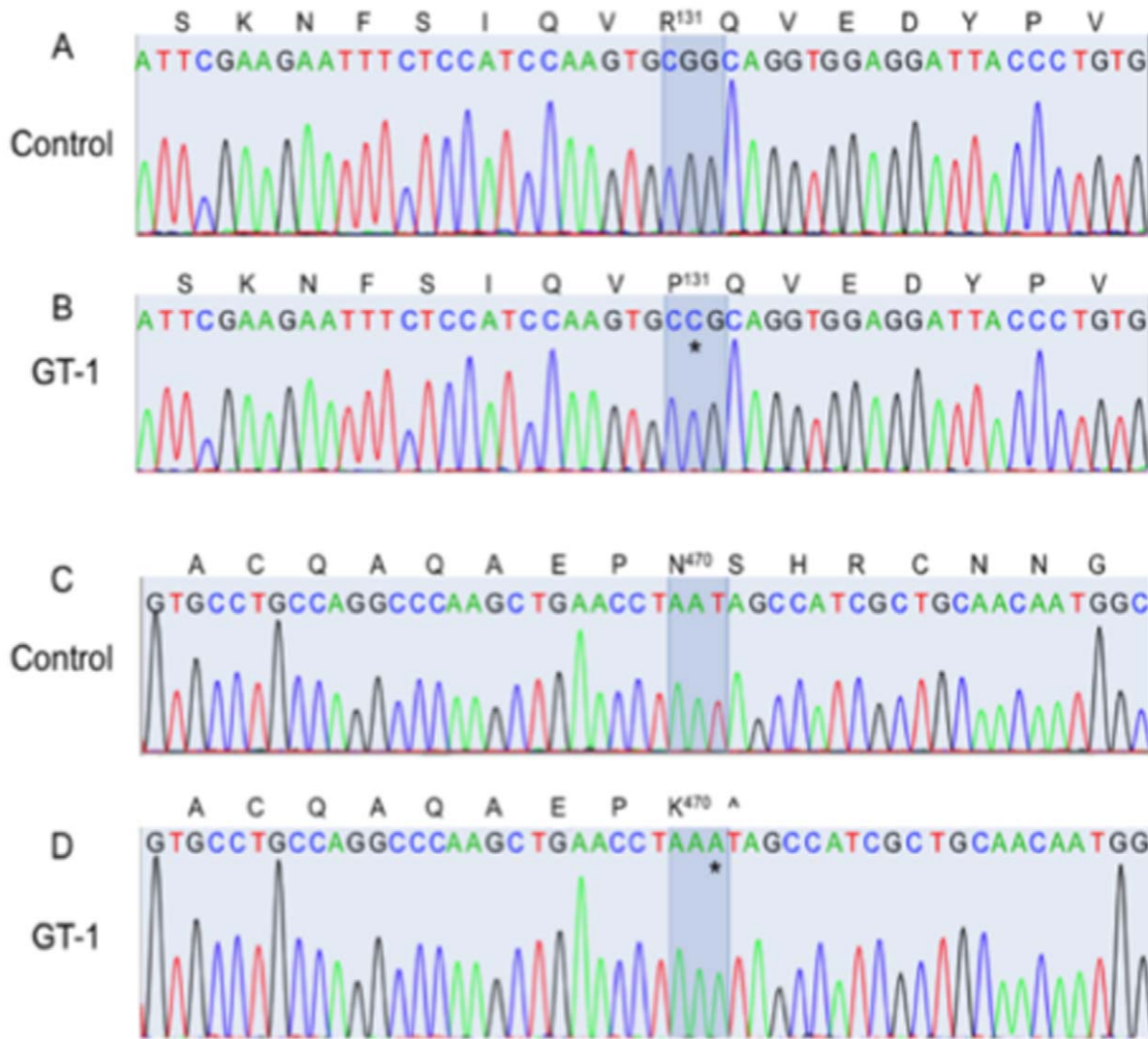


Figure 3. Nucleotide sequence of the mutated regions of the *ITGA2B* and *ITGB3* integrin genes in GT patients. (A–D) GT-1. In each case, the sequence data are displayed for one example PCR clone within the *ITGB3* gene in the genome, along with the readouts of the nucleotides of the translated products. No uncertainties were noted in any clones sequenced in these regions. The *ITGA2B* gene did not show mutations from WT *ITGA2B* in any region of the gene. (A) Normal human *ITGB3* sequence of the region coding for amino acids S¹²³–V¹³⁸ of WT α IIB. (B) The 2nd nucleotide (G) of the codon for R¹³¹ is mutated from G to C(*) in GT-1, thus altering R¹³¹ to P¹³¹ in the translated product. (C) Normal human *ITGB3* sequence of the region spanning amino acids A⁴⁶²–G⁴⁷⁷. (D) An insertion mutation of an A in the 3rd nucleotide (*) of the codon for N⁴⁷⁰ alters this amino acid to K⁴⁷⁰ and shifts the reading frame such that a stop codon (*) in the *ITGB3* gene of GT-1 replaces the WT amino acid, S⁴⁷¹. All protein sequences are numbered from Met¹ of the ORF of the protein. All corresponding nucleotide sequences are numbered from the 1st residue of the ATG translation initiation sequence.

doi:10.1371/journal.pone.0052878.g003

BSS-1, the homozygous abnormal *GPIBA* alleles of BSS-2, the *ITGB3* abnormal alleles in patient GT-1, and one abnormal *ITG2AB* allele of GT-2 have been deposited in the GenBank database. The accession numbers for the 5 sequences are KC120774–KC120778.

Clot Retraction Studies of GT Patients

Clot retraction performed on the GT specimens were variable. GT-1 (Figure 4A), showed no clot retraction after 30 min and instead revealed a homogeneous image without any distinctive contractile movement along the transverse plane, demonstrating impaired platelet function. Clot retraction of GT-2M (Figure 4B) whole blood was normal, while GT-2 (Figure 4C) showed weaker retraction tendencies (~2% of WT) than WT blood. The blood of

GT-3M (Figure 4D) was normal in this regard, and that of GT-3 (Figure 4E) showed ~50% of GT-3M retraction after 30 min. The weaker retraction properties of GT blood are due to the genetic functional attenuation of receptor α IIB/ β 3, which mediates platelet contraction and aggregation [16]. These three patients appear to have variable disease severity, as measured by clot retraction properties, with GT-1 the most profound example of GT, and GT-3 the least. This diversity in properties is likely due to the wide array of possible mutations present in α IIB and β 3.

FCA of the GT Platelets

Patient GT-1. PRP specimens from GT-1 were analyzed by FCA. A comparison of the FCA graphical representations of normal (N) PRP (Figure 4F) and GT-1 PRP (Figure 4G) shows a

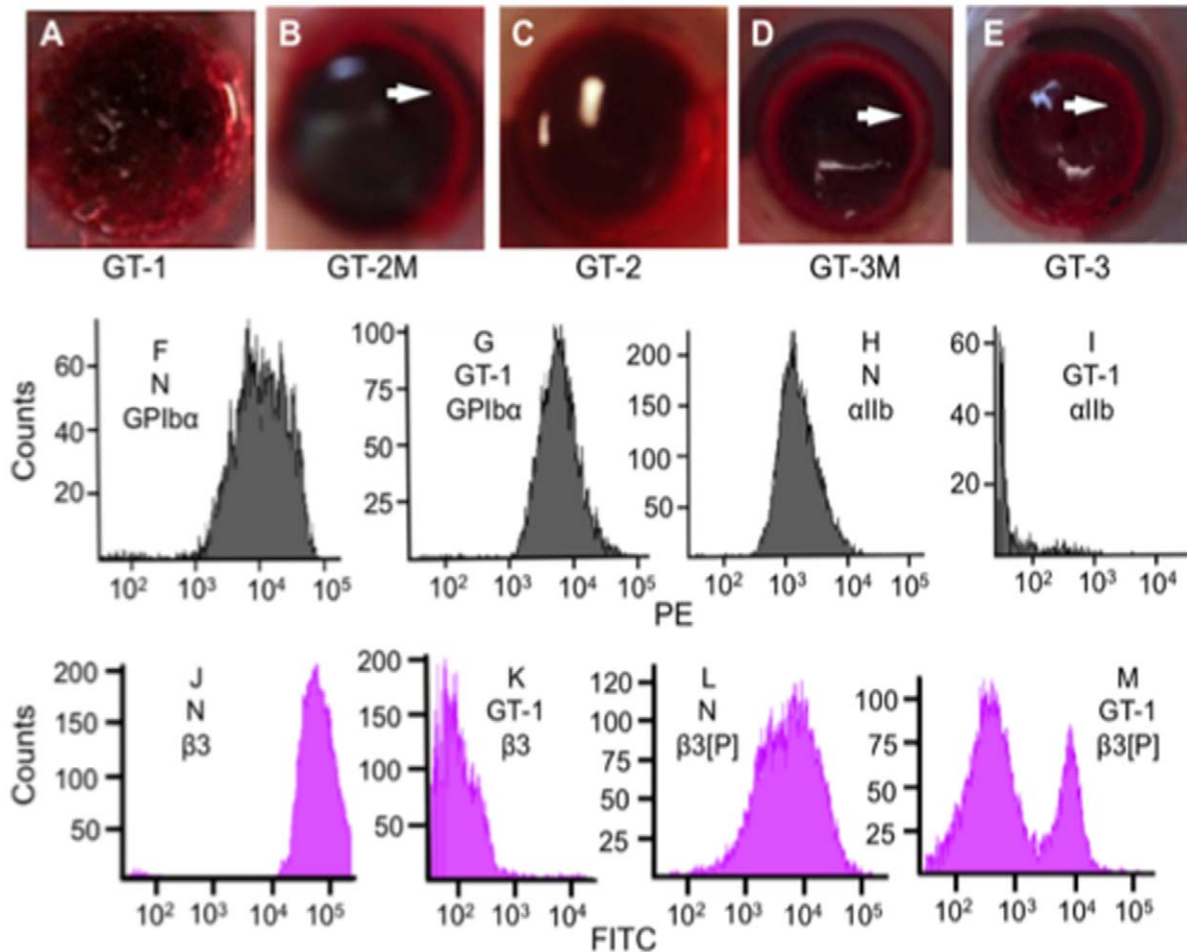


Figure 4. Platelets of GT patients. Whole blood clot retraction of (A) GT-1, (B) GT-2M, and (C) GT-2, (D) GT-3M, and (E) GT-3 clots. A ring of retraction (white arrows) is observed in GT-2M and GT-3M clots, whereas the GT-1, GT-2, and GT-3 specimens displayed much weaker retraction at 30 min. (F-M) Flow cytometric analysis of normal and GT-1 PRP. (F, G) Surface expression of GPIb α (CD42b) in (F) normal and (G) GT-1 platelets show similar expression levels of GPIb α . (H, I) Surface expression of integrin α IIb (CD41) in (H) normal and (I) GT-1 platelets show reduced expression of CD41 in GT-1 platelets, likely owing to the reduced levels of β 3 and thereby reduced amount of surface α IIb/ β 3 complexes. (J) Surface expression of integrin β 3 (CD61) in normal platelets from PRP shows one peak demonstrating the presence of integrin β 3 in the α IIb/ β 3 complex. (K) Surface expression of platelet β 3 of α IIb/ β 3 in GT-1 PRP shows a lack of reactivity of platelets with this antibody. (L) Surface expression of integrin β 3[740–769] (β 3[P]) in normal PRP. (M). Surface expression of integrin β 3[740–769] (β 3[P]) in GT-1 PRP. The downfield peak in (M) is similar to isotype controls and likely corresponds to the protein expressed by the truncated allele of integrin β 3 in α IIb/ β 3 in this patient. The smaller peak in (M) to the right shows a reactivity with the full-length allele of integrin β 3 in this complex, which harbors the [R131P] mutation but expresses the [740–769] peptide region of the protein.
doi:10.1371/journal.pone.0052878.g004

normal level of GPIb α . However, when compared to a normal control (Figure 4H), GT-1 displayed a near complete loss of reactivity of the antibody to integrin α IIb (Figure 4I), and was comparable in strength to the isotype IgG₁ control. Upon examination of integrin β 3 with a conformational antibody to β 3 in the α IIb/ β 3 complex, less than 5% of normal β 3 (Figure 4J) was evidenced in the platelets of GT-1 (Figure 4K). Another CD61 antibody, that recognizes the peptide region encompassing amino acids [740–769], reacts with control WT platelets (Figure 4L), but shows mixed reactivity in GT patients (Figure 4M). Since β 3 in GT-2 platelets has a stop codon at amino acid 471, the β 3 translated by this allelic DNA would not be expected to react with this antibody. This is borne out, as seen by one population in Figure 4M that is similar to the isotype control. However, the other allele of GT-1 platelets would translate a full-length mutated β 3 protein, which, if stably produced, would react with this antibody, as seen in the second upfield population of Figure 4M.

The results with these two antibodies are in agreement with the DNA sequencing that showed that this patient generates a mutated full-length β 3 on one allele and a truncated allele on the other, but the conformation of this protein is altered from the WT protein.

Patient GT-2. The platelets in the PRP of patient GT-2 also displayed normal levels of GPIb, when compared to samples taken from GT-2M, her biological mother (Figure 5A, B). However, reactivity to anti-integrin α IIb was very weak compared to her mother (Figure 5C, D). This suggests a significant loss of the surface native α IIb epitope in GT-2 platelets. Similarly, a loss in reactivity of the conformational epitope to anti-CD61 (β 3) is noted in the α IIb/ β 3 complex on the platelet surface of GT-2, as compared to the platelets of GT-2M (Figure 5E, F). With this antibody, one population displaying no antibody binding was observed, and a second upfield population displaying very weak antibody binding was also seen (Figure 5E, F). Similarly,

approximately 50% loss in reactivity to the linear C-terminal reactive antibody of $\beta 3$ (recognizing 740–769 amino acids of $\beta 3$) was observed in GT-2 (Figure 5H), when compared to reactivity of the GT-2M platelets (Figure 5G). However, the one subset of platelets (50%) in GT-2 remains, with a native reactivity to the linear C-terminus of $\beta 3$, as observed by the upfield peak in Figure 5H. These data demonstrate that full-length $\beta 3$ is present in the platelets of patient GT-2.

Patient GT-3. The platelets of GT-3M and GT-3 essentially showed the same FCA properties (Figure 5I-P) with these antibodies when compared to GT-2M and GT-2, with only qualitative differences between the paired samples.

TEG Analysis of Normal Human Whole Blood Clotting

We considered the values of R, K_{20} , A, MA_{max} , LY_{30} , and LY_{60} (Figure 6A, inset) in recalcified plasma of control samples (Figure 6A; Table 2), as basal measures of overall normal hemostasis balance in whole blood. It is seen that the fibrin formed in heparin/reptilase/hFXIIIa (Figure 6C), absent thrombin-induced platelet involvement, has very low viscoelastic strength, as reflected by the MA_{max} value (Figure 6C; Table 2). Thus, MA_F is minimal (Figure 6C; Table 2). Additionally, in the case of a fibrinogen deficiency, activated platelets, alone, do not provide a thrombus that is of measurable viscoelastic strength, with MA values being essentially zero [17]. These data suggest that both functional platelets and fibrinogen are critical to development of a stable viscoelastic thrombus. Regarding fibrinolysis, the

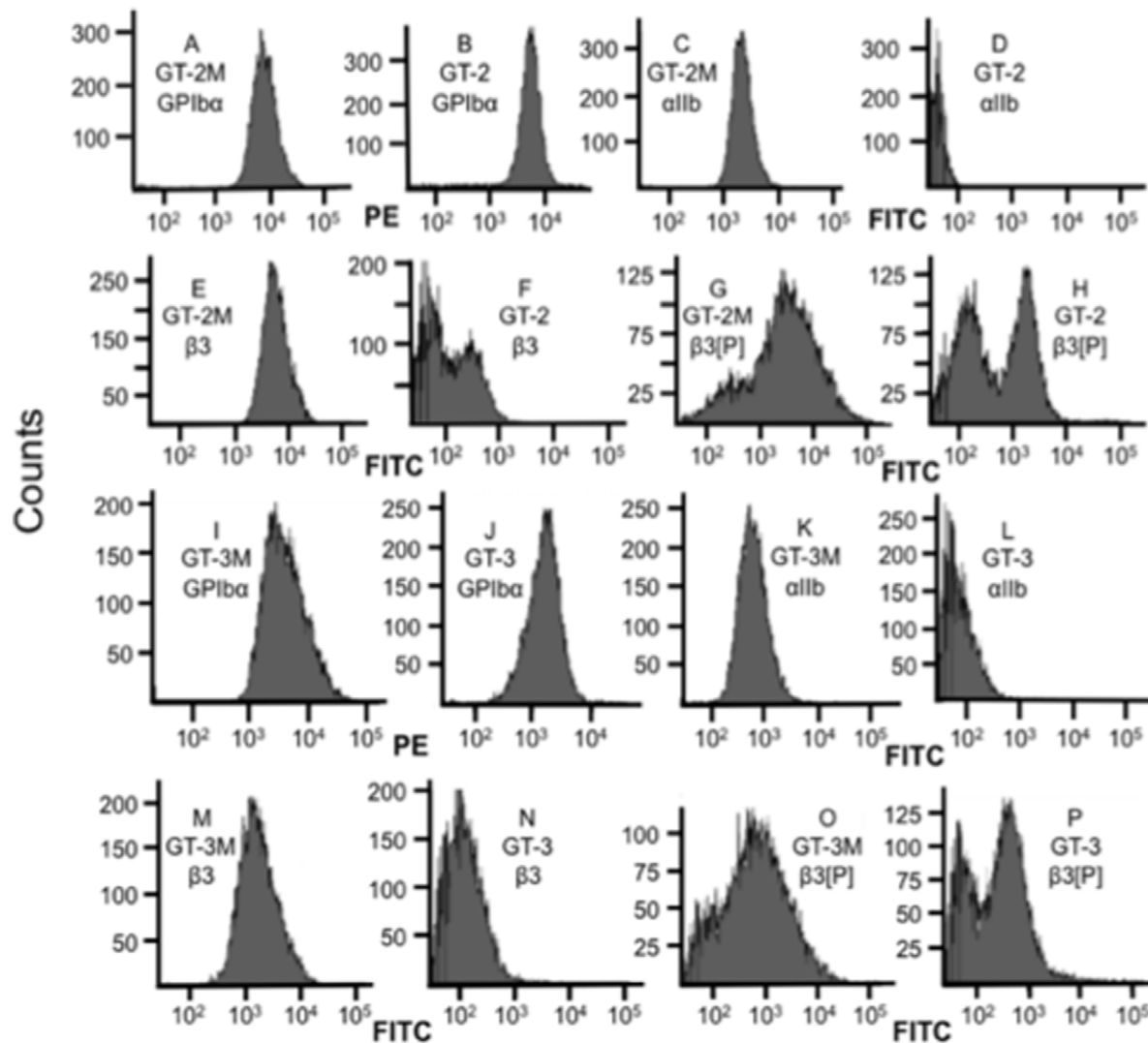


Figure 5. FCA of platelets from PRP of symptomatic GT-2 and GT-3 patient blood, and their heterozygous mothers (GT-2M and GT-3M, respectively). (A–H) Analysis on the PRP of GT-2 and her heterozygous mother (GT-2M). Normal expression of GPIIb/IIIa is seen in (A) GT-2M and (B) GT-2. Integrin $\alpha IIb/\beta 3$ is expressed on platelets of (C) GT-2M, but not (<5%) expressed on the platelets of (D) GT-2. Integrin $\beta 3$ in the $\alpha IIb/\beta 3$ complex is expressed on platelets of (E) GT-2M, but not (<5%) expressed on the platelets of (F) GT-2. The amino-terminal peptide [residues 740–769] of $\beta 3$ ($\beta 3[P]$) is expressed on the platelets of (G) GT-2M and partly expressed (<10%) on platelets of (H) GT-2 (upfield peak), with another peak (downfield) of weak expression on GT-2. (I, J) Expression of GPIIb/IIIa is similar in GT-3M and GT-3, whereas (K, L) expression of αIIb is greatly attenuated in GT-3, compared to GT-3M. (M, N) Similarly, integrin $\beta 3$ in $\alpha IIb/\beta 3$ displays greatly reduced expression in GT-3 compared to GT-3M. (O, P) The C-terminal peptide region of $\beta 3$ is recognized in GT-3M, and only partly recognized GT-3 (likely maternal allele), suggesting that a truncation of $\beta 3$ is present in one allele (likely paternal) in the patient. doi:10.1371/journal.pone.0052878.g005

activation state (-tPA) or potential activation state (+tPA \pm EACA) of the fibrinolytic system, as reflected by LY₃₀ and/or LY₆₀, are employed as diagnostic measures of pathological fibrinolysis in individuals, while also reporting the overall competency of the fibrinolytic system. The values for normal blood are provided in Table 2, as obtained from traces, such as in Figure 6B.

These concepts were expanded by analyses of rates, levels, and strength of thrombus formation after additions of other components of the clotting cascade to blood samples. R-values were greatly decreased upon addition of Ca²⁺/thrombin, and thrombi of high viscoelastic strength were formed (Figure 6A; Table 2). In this case, the MA_{max} achieved was not optimal since the high

thrombin level initially present likely affected the strength of the thrombus, possibly resulting from the alteration of strand assembly dynamics of the fibrin via the more rapid formation of fibrin by exogenous thrombin [18,19]. Thrombi formed with Ca²⁺/kaolin provided thromboelastogram-derived values that were only slightly altered from those of Ca²⁺, alone (Figure 6A; Table 2). This shows that the intrinsic pathway is operating to near maximal capacity in maintenance of basal hemostasis and does not accelerate or stabilize thrombi upon further addition of kaolin. However, addition of Ca²⁺/sTF/kaolin to blood resulted in much lowered R and K₂₀ values and provided a high MA_{max} (Figure 6A, Table 2), demonstrating that the TF pathway is likely not highly functional

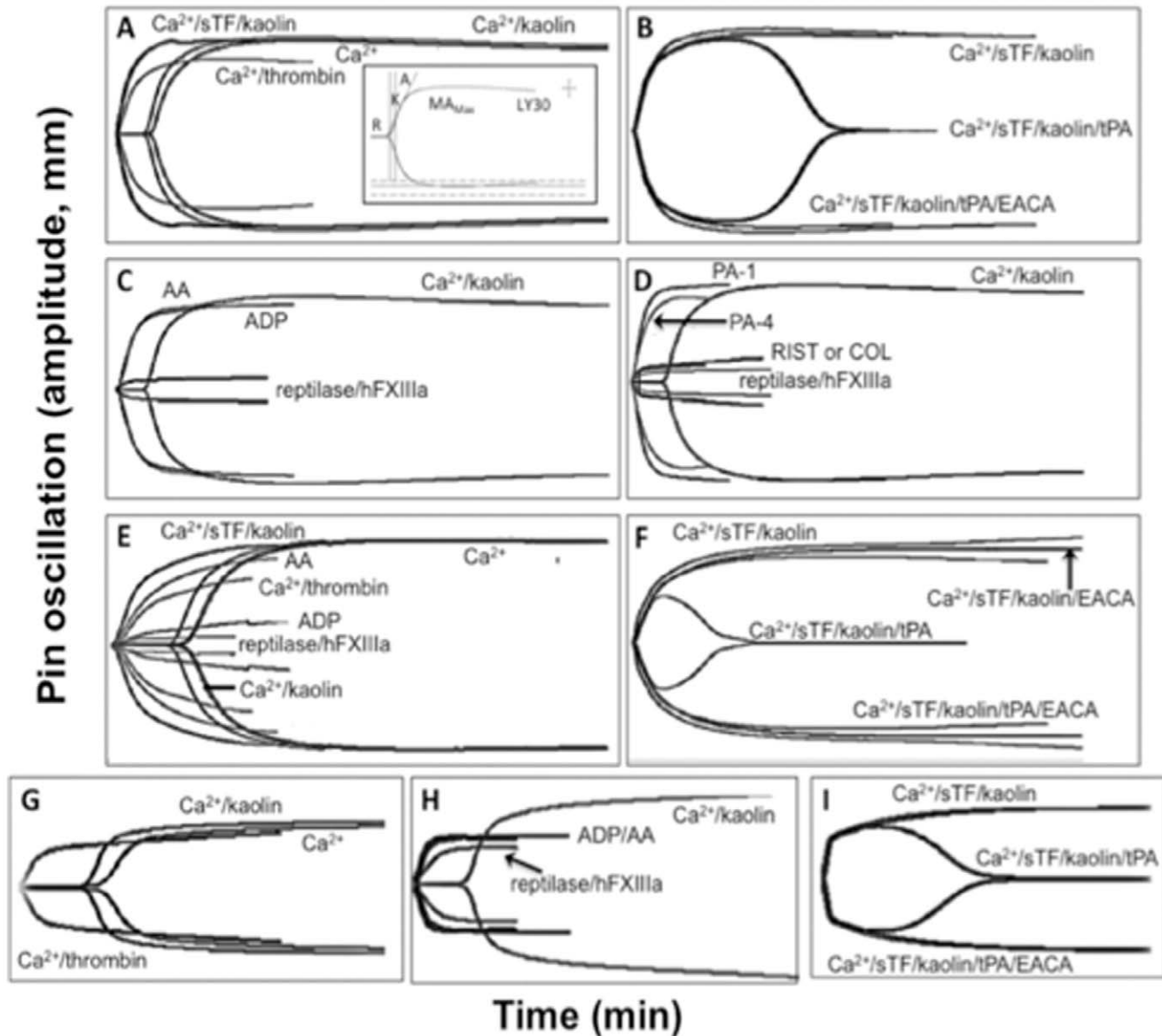


Figure 6. Representative TEG traces of human whole blood. (A–D) Representative normal control. Samples were collected in citrate-containing plastic tubes for additions of (A) Ca²⁺, Ca²⁺/kaolin, Ca²⁺/sTF/kaolin, or Ca²⁺/thrombin; (B) Ca²⁺/sTF/kaolin/tPA or Ca²⁺/sTF/kaolin/tPA/EACA, compared to the trace with Ca²⁺/sTF/kaolin/tPA. Samples were collected in heparin-containing plastic tubes and used for platelet stimulation of the MA_F generated by (C) reptilase/hFXIIIa with AA or ADP; or (D) COL, RIST, PA-1, or PA-4. The MA_{max} obtained (from A) with Ca²⁺/kaolin was used as the 100% reference to compare all agonists for calculation of the degree of agonist stimulation. The inset in Figure 6A displays the parameters that were calculated by the software. (E–I) Similar measurements for (E, F) BSS-2 and (G–I) GT-1 whole blood, collected under the same conditions as normal control blood.

doi:10.1371/journal.pone.0052878.g006

Table 2. Whole blood TEG parameters.

Human	R (min)	K ₂₀ (min)	A (degrees)	MA _{max} (mm)	LY ₃₀ (%)	LY ₆₀ (%)
Controls^a						
Ca ²⁺	9.6±0.6	2.6±0.2	56±3	62±2	0	<2
Ca ²⁺ /kaolin	7.3±0.4	2.1±0.2	59±3	63±2	0	<2
Ca ²⁺ /sTF/kaolin	0.8±0.1	1.2±0.2	75±2	64±2	2.5±1.1	5.0±0.7
Ca ²⁺ /sTF/kaolin/htPA	0.6±0.1	1.5±0.2	72±2	62±3	48±7	75±3
Ca ²⁺ /thrombin	0.8±0.1	2.8±0.3	60±4	45±4	0	<2
Reptilase/hFXIIIa	1.2±3	nd	nd	5.4±0.8	nd	nd
BSS-1^c						
Ca ²⁺	10.6; 18	5.8; 4.4	34; 41	54; 59	0	<2
Ca ²⁺ /kaolin	7.7; 14.9	2.3; 3.4	57; 47	63; 60	0	<2
Ca ²⁺ /sTF/kaolin	0.8; 1.1	2.5; 2.7	71; 63	62; 57	0	<2
Ca ²⁺ /sTF/kaolin/htPA	0.3	4.8	71	26	49	74
Ca ²⁺ /thrombin	0.8; 0.8	6.2; 5.4	37; 40	46; 49	0	<2
Reptilase/hFXIIIa	0.8; 2.2	nd	16; 17	8; 4	0	0
BSS-2^c						
Ca ²⁺	11; 5.7	2.7; 1.7	56; 68	71; 76	0; 0	<2; <2
Ca ²⁺ /kaolin	8.6; 5.4	2.5; 1.7	58; 54	75; 77	0; 0	<2; <2
Ca ²⁺ /sTF/kaolin	0.7; 0.8	1.1; 1.6	78; 73	74; 69	0; 0	<2; <2
Ca ²⁺ /sTF/kaolin/htPA	0.2; 0.7	1.7; 1.6	69; 72	37; 37	77; 87	74; 100
Ca ²⁺ /thrombin	0.8; 0.6	3.5; 2.2	53; 65	63; 74	0; 0	<2; <2
Reptilase/hFXIIIa	0.9; 0.5	nd; nd	27; 55	7; 10	nd; nd	nd; nd
GT-1^c						
Ca ²⁺	9.0; 12	3.4; 9.8	52; 35	25; 21	0; 0	0; 0
Ca ²⁺ /kaolin	6.9; 8.6	2.5; 3.5	39; 23	32; 28	0; 0	0; 0
Ca ²⁺ /sTF/kaolin	0.8; 1.0	1.8; 4.9	77; 62	30; 27	0; 0	0; 0
Ca ²⁺ /sTF/kaolin/htPA	0.3; 0.6	2.1	75; 72	23; 15	72; 88	86; 93
Ca ²⁺ /thrombin	0.5; 1.2	nd; nd	55; 35	18; 17	0; 0	0; 0
Reptilase/hFXIIIa	0.6; 0.5	nd; nd	51; 67	15; 15	nd; nd	nd; nd
GT-2						
Ca ²⁺	10	6	36	30	0	0
Ca ²⁺ /kaolin	5.1	4.6	51	34	0	0
Ca ²⁺ /sTF/kaolin	0.9	5.4	64	36	0	0
Ca ²⁺ /sTF/kaolin/htPA	0.9	5.7	65	25	81	91
Ca ²⁺ /thrombin	1.1	nd	32	13	0	0
Reptilase/hFXIIIa	0.7	nd	57	10	nd	nd
GT-3						
Ca ²⁺	4.8	1.8	66	67	0.2	nd
Ca ²⁺ /kaolin	3.8	1.6	67	66	0.5	nd
Ca ²⁺ /sTF/kaolin	0.9	1.8	69	64	1.1	nd
Ca ²⁺ /sTF/kaolin/htPA	0.6	1.6	75	27	95	nd
Ca ²⁺ /thrombin	0.8	4.5	46	47	0	nd
Reptilase/hFXIIIa	0.3	nd	53	21	nd	nd

^aNormal human controls, N = 10.

^b[htPA] = 200 ng/ml.

^cData are from separate blood draws >4 months apart.

nd, not determined.

doi:10.1371/journal.pone.0052878.t002

in basal hemostasis and likely provides a rapid response mechanism to injury. Lastly, unstimulated LY₃₀ and LY₆₀ values were very low in control blood (Figure 6B, Table 2), suggesting a minor degree of basal fibrinolysis in healthy individuals. With thrombi rapidly formed by Ca²⁺/sTF/kaolin, inclusion of htPA (200 ng/ml) to human blood resulted in complete lysis (Figure 6B). Further, addition of EACA to Ca²⁺/sTF/kaolin/htPA completely inhibited the lysis of whole blood thrombi (Figure 6B).

Platelets Provide Viscoelastic Strength to the Human Thrombus in Normal Plasma

In the case of TEG-based platelet functional analysis of normal human whole blood, the MA_A is measured in heparin/reptilase/hFXIIIa blood after addition of a platelet activator (e.g., ADP, AA, RIST, COL, PA-1, PA-4). In these experiments, fibrin is formed by reptilase, which is very similar to that formed by thrombin [20], and crosslinked by exogenous FXIIIa, and any thrombin

generated is inhibited by heparin/antithrombin III. Different platelet activators are then added, and the MA_{max} determined. The MA ratios (with the MA_F subtracted), with and without platelet activators, allowed assessment of the effectiveness of the individual platelet agonists to stimulate the assembly of strong whole blood thrombi. The data obtained for the human controls (Figure 6C, D; Table 3) show that the agonists, ADP and AA (Figure 6C), as well as the PAR-1 and PAR-4 agonist peptides, PA-1, and PA-4, respectively (Figure 6D), result in thrombi of strong viscoelasticity. However, RIST and COL do not allow thrombi of high strength to be formed (Figure 6D) at concentrations of each that effectively aggregate platelets in whole blood (Figure 7C,E, Table 4), when aggregation is measured independently of thrombus formation.

Table 3. Platelet mapping by TEG.

Human	ADP ^c (%) 2 μ M ^d	AA ^c (%) 1 mM ^d	RIST ^c (%) 0.3 mg/ml ^d	COL ^c (%) 3.2 μ g/ml ^d	PA-1 ^c (%) 31 μ M ^d	PA-4 ^c (%) 663 μ M ^d
Controls ^a	78 \pm 4	99 \pm 2	4 \pm 2	5 \pm 2	84 \pm 6	73 \pm 6
BSS-1 ^b	22; 36	62; 66	-6.4; 0	-4.4; 1	48	32
BSS-2 ^b	20; 5	92; 90	-1.3; 0	0.5; 0	84; 60	64; 71
GT-1 ^b	22; 0	26; 0	7; 0	0; 3	14; 0	0; 0
GT-2	0	37	0	0	20	0
GT-3	68	0	0	21	69	76

^aNormal human controls, N = 10.

^bData are from separate blood draws >3 months apart.

^cThe stimulation by each of these agents with respect to the MA of Ca²⁺/kaolin (= 100%).

^dFinal concentration in the reaction vessel.

doi:10.1371/journal.pone.0052878.t003

TEG and Platelet Aggregometry Analyses of BSS and GT Whole Blood Clotting

There are differences between whole blood thrombus stability in normal and BSS-derived whole blood, but some differences between the two BSS patients are also seen (Table 2), probably due to the disparate nature of the deficiencies in each case. Upon recalcification of citrated blood, the R and K₂₀ are slightly prolonged in BSS-1 samples, and less so in BSS-2 blood (Figure 6E; Table 2). This indicates a defective level of functional thrombin in these patients, undoubtedly due to the thrombocytopenia and the large platelet surface areas. Both of these factors would attenuate the levels and availability of the prothrombinase complex on platelets. This hypothesis is fortified by the large decrease in R after addition of Ca²⁺/thrombin (Figure 6E, Table 2). K₂₀ is not affected in this situation because new thrombin is not formed at a more rapid rate when Ca²⁺/thrombin is added. However, the R and K₂₀ of BSS whole blood (BSS-2 is shown as the example) are greatly decreased after addition of Ca²⁺/sTF/kaolin (Figure 6E, Table 2). As with normal whole blood, addition of Ca²⁺/kaolin did not remarkably alter these TEG parameters, again showing that the intrinsic system functions to maintain basal hemostasis in the individual. Thus, despite low platelet counts and large platelets, strong viscoelastic thrombi are formed with BSS platelets in whole blood. As with normal controls, no unstimulated fibrinolysis occurred in BSS blood (Figure 6F, Table 2), but addition of htPA (200 ng/ml) to BSS blood resulted in complete lysis, a process also nearly completely inhibited by EACA (Figure 6F).

Platelet functionality in whole blood thrombus formation, as analyzed by TEG, is remarkable in that ADP stimulation of BSS platelets is defective with regard to generating strong viscoelastic thrombi with fibrin (Figure 6E, Table 3), compared to control blood, despite the finding that ADP leads to near normal impedance-based aggregation of BSS platelets (Figure 7A, F, K; Table 4). On the other hand, AA stimulation of the MA_F is similar to that of normal blood (Figure 6E; Table 3), as is the impedance-based aggregation of these platelets (Figure 7B, G, L; Table 4). As expected, there was severe attenuation of platelet aggregation with RIST in the BSS patients compared to normal blood (Figure 7E,J,O; Table 4), but other platelet activators tested (AA, COL, PA-1, and PA-4; example provided for PA-1 in Figure D, I, N) appeared quantitatively similar to the blood of normal controls (Table 4).

Regarding GT whole blood clotting, values of R, K₂₀, and A in recalcified blood were similar to WT control blood (Figure 6G, H; Table 2). The response of these values to thrombus formation with Ca²⁺/kaolin, Ca²⁺/thrombin, and Ca²⁺/sTF/kaolin were also

similar to WT controls. This indicates that platelets were activated by thrombin in GT blood and could assemble into a thrombus. However, as reflected by the substantially lower MA_{max} value (Figure 6G, Table 2), platelet/fibrin interactions were affected and assemble into a substantially weaker thrombus, whether the platelets were activated by thrombin (Figure 6G, Table 2); ADP, AA (Figure 6H); or ristocetin, collagen, PA-1, or PA-4 (not shown). In separate aggregation studies, of all the platelet activators examined, only collagen weakly stimulated aggregation, likely via binding to a separate receptor on platelets. Ristocetin did not function in this manner in aggregation assays, despite the functional presence of GP1b (Figure 7, Table 4).

The thrombi formed in the GT whole blood did not show spontaneous clot lysis, but did display very strong lysis with htPA (Figure 6I, Table 2), in a process that was effectively inhibited by EACA. Perhaps the more rapid lysis of the clots in GT blood displayed at 30 min (Table 2) is due to the weakened clots formed in this system.

Discussion and Conclusions

While it is difficult to recapitulate in vivo hemostasis in ex vivo models, nonetheless much has been learned that is clinically applicable over decades of efforts in this regard. Studies of hemostasis mechanisms in plasma have focused on the role of soluble factors in fibrin formation. However, it is relevant to expand hemostasis mechanistic studies to whole blood to include the role of platelets in clinical consideration of the hemostasis status of patients. A manner of understanding the features of platelets needed to form stable thrombi is to study whole blood that contains platelets with known deficiencies. BSS patients afford one such opportunity. In this case, the contributions of GP1b in whole blood thrombus formation can be studied in the absence of high shear. However, the numbers of these patients are very limited (1:1,000,000), and only ~100 cases have been confirmed in the literature. Fortunately, we were able to access two BSS patients for this work. Deficiencies in human GP1b, both genetic and acquired, are found in BSS [21], cardiopulmonary bypass (CPB) [22] surgery, and surgical trauma [23], and in targeted transgenic mice [24], and lead to bleeding diatheses, presumably due to defects in the binding of platelets to the subendothelium. Whether such a deficiency would alter rates of thrombus formation and ultimate strength of the thrombus in whole blood with exogenous soluble subendothelium components, was not known, and is one contribution from this work.

Severe attenuation, of human GP1b expression, as in the case of BSS, leads to macrothrombocytopenia, but this has minimal

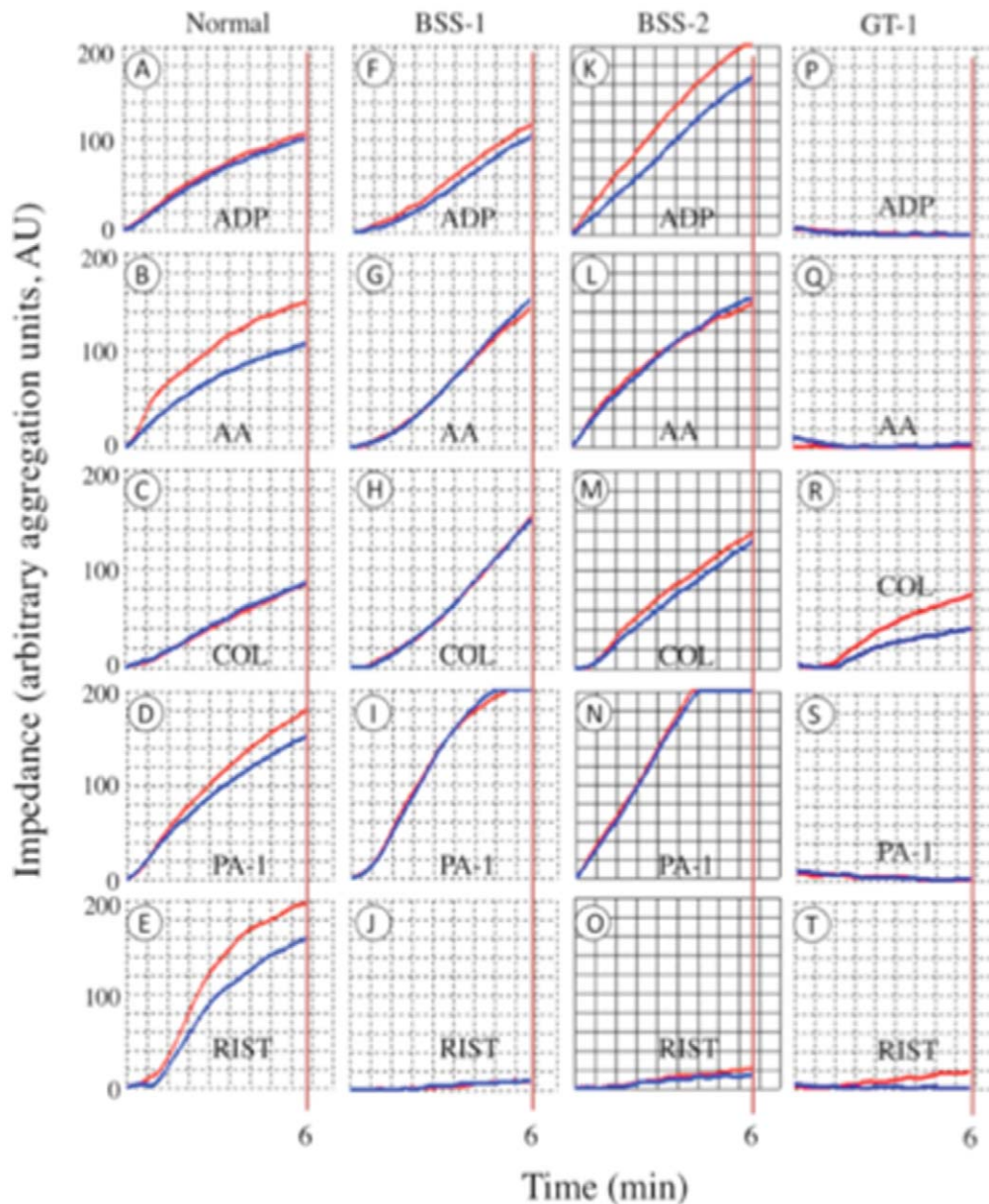


Figure 7. Human whole blood platelet aggregation measurements. The increase in impedance of platelets aggregated on multiplate sensors and transformed by software into arbitrary aggregation units is plotted against time. Curves are generated for 6 min and the areas under the curve, from 0–6 min, are calculated by the software as a measure of platelet aggregation. Two independent runs were generated for each agonist (blue and red curves in each panel) and the mean of the areas was employed. The agonists are listed on each panel. Data were collected on normal human whole blood, and on BSS-1, BSS-2, and GT-1 blood.
doi:10.1371/journal.pone.0052878.g007

effects on overall plasma-based coagulation markers. In humans, TEG-based whole blood coagulation parameters are also not substantially affected whether thrombin or a direct pharmacological agonist of downstream PAR-1 activation is employed as the overall activator of platelets. However, when thrombin is blocked and other platelet activators are used to induce thrombus assembly in the presence of fibrin, the results are somewhat surprising. In normal human plasma, RIST and COL aggregate and probably activate platelets, but stable viscoelastic thrombi are minimally formed. On the other hand, ADP and AA both aggregate control platelets and allow normal thrombus assembly. In human BSS blood, AA functions normally, but the effects of ADP on thrombus assembly and/or stability are greatly attenuated compared to

normal controls. The fact that direct activation of PAR-1 by PA-1 reverses the weakened stimulation by ADP of the MA_F in BSS whole blood links ADP stimulation of thrombi of high viscoelastic strength to PAR-1 activation.

Confirmation of the importance of the fibrin(ogen)-binding integrin, α IIb/ β 3, in assembling a thrombus has been obtained by examination of the blood of human GT patients. GT-1 is shown as the example, an individual who possessed a rare double heterozygous GPIb mutation that inactivated this receptor. This GT blood did not show effective platelet aggregation with a series of platelet activators, except weakly in the case of collagen, and did not assemble with fibrin into a strong viscoelastic clot. Thus, thromboelastograms obtained on patients with deficiencies or

Table 4. Impedance-based platelet aggregometry (AU) of the study groups^a.

Human ^b	ADP 6.5 μM^d	AA 0.5 mM ^d	RIST 0.88 mg/ml ^d	COL 3.2 $\mu\text{g/ml}^d$	PAR-1 32 μM^d	PAR-4 663 μM^d
Controls ^b	125 \pm 10	143 \pm 10	146 \pm 8	136 \pm 10	195 \pm 47	213 \pm 8
BSS-1 ^c	109; 93; 92	147; 148; 121	10; 0; 8	150; 149; 84	219; 182; 165	161; 153
BSS-2 ^c	187; 146; 168	150; 137; 150	18; 37; 37	134; 60; 124	272; 199	162; 171
GT-1 ^c	0; 0	0; 0	10; 0	57; 85	0; 5	0
GT-2	0	105	74	163	5	5
GT-3	29	43	95	69	42	39

^aTwo analyses were performed for each agonist in all cases. Data are reported as the mean value of the areas under the respective curves.

^bNormal human controls, N = 10.

^cData are from separate blood >4 months apart.

^dFinal concentration in the reaction vessel.

doi:10.1371/journal.pone.0052878.t004

blocks of $\alpha\text{IIb}/\beta_3$, would manifest in very low MA_{max} values. Qualitatively similar results are seen with 2 other GT patients with different mutations. Thus, while general principles can be established with an array of BSS and GT patients, given the array of possible mutations that lead to BSS and GT, it is suggested that each patient is examined individually.

Overall, the results demonstrate that human platelet activation, as measured by the ability of platelets to aggregate, does not necessarily translate to the assembly of a thrombus of high viscoelastic strength, and further suggests that the platelet receptors engaged for activation are mechanistically related to the nature of the platelet-fibrin assembly that is measured by clot strength. The contribution of platelet defects, and specifically that of attenuation of GPIb expression [25], to whole blood hemostasis has been a long-standing consideration in on-pump CPB surgery, where TEG analysis on whole blood is employed to predict post-surgical bleeding [26,27], and off-pump coronary artery bypass surgery led to lower platelet activation defects than on-pump surgery [28].

These factors may also be applicable to the coagulopathy of traumatic brain injury [29–34], wherein ADP stimulation of platelets to assemble into a thrombus is diminished, as is expression of platelet surface GPIb [23], but AA stimulation of thrombus formation is affected to a lesser degree [35]. As with the high mechanical shear forces to which platelets are exposed in CPB, high tissue shear forces are also present in certain types of severe TBI, e.g., inertial injury, and can result in excess vWF-dependent activation and possible shedding of the ectodomain of GPIb [36,37]. Thus, platelets might be generated in severe TBI that are GPIb α deficient, as in BSS. Therefore, BSS platelets are not only critical to understand the mechanistic role of GPIb α in platelet aggregation and thrombus strength, but may also model some of the platelet dysfunctions in the hypocoagulopathy of TBI and CPB, and other maladies.

The results of this study segregate platelet activation, reflected by platelet aggregation, from that represented by assembly into

thrombi of high viscoelastic strength, and suggest that the nature of the thrombus formed depends on the receptors and signaling mechanisms that are engaged. ADP stimulation of thrombus formation is a particularly sensitive indicator of the nonsingularity of platelet activation. These findings have implications in treatment of platelet-based coagulopathies, e.g., CPB and TBI, and suggest that platelet counts and platelet aggregation tests, alone, may not sufficiently correlate with effective thrombus formation, and patients, who appear normal in these regards, may still benefit from platelet replacement therapy. More specifically, in the case of coagulopathic patients, thromboelastographic analysis of whole blood thrombus formation and stability is an effective guide for goal-directed administration of blood products [35].

Acknowledgments

We thank the staff of the Freimann Life Sciences Facility for the breeding and husbandry of mice and the phlebotomy team at Memorial Hospital of South Bend for individual blood collection. The cooperation of the Aurora Clinic in our obtaining some of the blood samples is also gratefully acknowledged. We also thank Dr. Robert M. Montgomery, Blood Center of Wisconsin, Dr. Amy D. Shapiro, Indiana Hemophilia & Thrombosis Center, and Dr. Mortimer Poncz, Children's Hospital of Pennsylvania, Carol A. Diamond, University of Wisconsin, and David L. Green and Michael Nardi, New York University, for identifying some of the BSS and GT patients. The TEG equipment was donated by Haemonetics, Inc., and some of the reagent expenses were defrayed by this same company. Similarly, the Multiplate apparatus and some reagents were provided by Verum Diagnostica.

Author Contributions

Conceived and designed the experiments: FJC VAP MW. Performed the experiments: ZL PKD RDB HM DLD DLS MJS. Analyzed the data: FJC ZL PKD RDB HM DLD DLS MJS VAP MW. Wrote the paper: FJC VAP.

References

- Ruggeri ZM (1997) Mechanisms initiating platelet thrombus formation. *Thromb Haemost* 78: 611–616.
- Sugiyama T, Okuma M, Ushikubi F, Sensaki S, Kanaji K, et al. (1987) A novel platelet aggregating factor found in a patient with defective collagen-induced platelet aggregation and autoimmune thrombocytopenia. *Blood* 69: 1712–1720.
- Ezumi Y, Uchiyama T, Takayama H (2000) Molecular cloning, genomic structure, chromosomal localization, and alternative splice forms of the platelet collagen receptor glycoprotein VI. *Biochem Biophys Res Commun* 277: 27–36.
- Nuytens BP, Thijs T, Deckmyn H, Broos K (2011) Platelet adhesion to collagen. *Thromb Res* 127: S26–S29.
- Jackson SP, Nesbitt WS, Kulkarni S (2003) Signaling events underlying thrombus formation. *J Thromb Haemost* 1: 1602–1612.
- Dorsam RT, Kunapuli SP (2004) Central role of the P2Y12 receptor in platelet activation. *J Clin Invest* 113: 340–345.
- Brass LF, Manning DR, Cichowski K, Abrams CS (1997) Signaling through G proteins in platelets: to the integrins and beyond. *Thromb Haemost* 78: 581–589.
- Lopez JA, Andrews RK, Afshar-Kharghan V, Berndt MC (1998) Bernard-Soulier syndrome. *Blood* 91: 4397–4418.

9. Lopez JA, Ludwig EH, McCarthy BJ (1992) Polymorphism of human glycoprotein Ib alpha results from a variable number of tandem repeats of a 13-amino acid sequence in the mucin-like macroglycopeptide region. Structure/function implications. *J Biol Chem* 267: 10055–10061.
10. Kaski S, Kekomaki R, Partanen J (1996) Systematic screening for genetic polymorphism in human platelet glycoprotein Ibalpha. *Immunogenetics* 44: 170–176.
11. Kuijpers RW, Faber NM, Cuypers HT, Ouweland WH, von dem Borne AE (1992) NH2-terminal globular domain of human platelet glycoprotein Ib alpha has a methionine 145/threonine145 amino acid polymorphism, which is associated with the HPA-2 (Ko) alloantigens. *J Clin Invest* 89: 381–384.
12. Afshar-Kharghan V, Lopez JA (1997) Bernard-Soulier syndrome caused by a dinucleotide deletion and reading frameshift in the region encoding the glycoprotein Ib alpha transmembrane domain. *Blood* 90: 2634–2643.
13. Kenny D, Newman PJ, Morateck PA, Montgomery RR (1997) A dinucleotide deletion results in defective membrane anchoring and circulating soluble glycoprotein Ib alpha in a novel form of Bernard-Soulier syndrome. *Blood* 90: 2626–2633.
14. Kenny D, Jonsson OG, Morateck PA, Montgomery RR (1998) Naturally occurring mutations in glycoprotein Iba that result in defective ligand binding and synthesis of a truncated protein. *Blood* 92: 175–183.
15. Burset M, Seledtsov IA, Solovyev VV (2000) Analysis of canonical and non-canonical splice sites in mammalian genomes. *Nucl Acids Res* 28: 4364–4375.
16. Basani RB, Vilare G, Shattil SJ, Kolodziej MA, Bennett JS, et al. (1996) Glanzmann thrombasthenia due to a two amino acid deletion in the fourth calcium-binding domain of alpha IIb: demonstration of the importance of calcium-binding domains in the conformation of alpha IIb beta 3. *Blood* 88: 167–173.
17. Castellino FJ, Donahue DL, Navari RM, Ploplis VA, Walsh M (2011) An accompanying genetic severe deficiency of tissue factor protects mice with a protein C deficiency from lethal endotoxemia. *Blood* 117: 283–289.
18. Wolberg AS, Allen GA, Monroe DM, Hedner U, Roberts HR, et al. (2005) High dose factor VIIa improves clot structure and stability in a model of haemophilia B. *Br J Haematol* 132: 645–655.
19. Wolberg AS, Monroe DM, Roberts HR, Hoffman M (2003) Elevated prothrombin results in clots with an altered fiber structure: a possible mechanism of the increased thrombotic risk. *Blood* 101: 3008–3013.
20. Carr ME, Gabriel DA, McDonagh J (1986) Influence of Ca²⁺ on the structure of reptilase-derived and thrombin-derived fibrin gels. *Biochem J* 239: 513–516.
21. Jenkins CS, Phillips DR, Clemetson KJ, Meyer D, Larrieu MJ, et al. (1976) Platelet membrane glycoproteins implicated in ristocetin-induced aggregation. Studies of the proteins on platelets from patients with Bernard-Soulier syndrome and von Willebrand's disease. *J Clin Invest* 57: 112–124.
22. Rinder CS, Gaal D, Student LA, Smith BR (1994) Platelet-leukocyte activation and modulation of adhesion receptors in pediatric patients with congenital heart disease undergoing cardiopulmonary bypass. *J Thorac Cardiovasc Surg* 107: 280–288.
23. Bunesco A, Widman J, Lenkei R, Menyes P, Levin K, et al. (2002) Increases in circulating levels of monocyte-platelet and neutrophil-platelet complexes following hip arthroplasty. *Clin Sci* 102: 279–286.
24. Ware J, Russell S, Ruggeri ZM (2000) Generation and rescue of a murine model of platelet dysfunction: the Bernard-Soulier syndrome. *Proc Natl Acad Sci USA* 97: 2803–2808.
25. Maquelin KN, Berckmans RJ, Nieuwland R, Schaap MCL, ten Have K, et al. (1998) Disappearance of glycoprotein Ib from the platelet surface in pericardial blood during cardiopulmonary bypass. *J Thorac Cardiovasc Surg* 115: 1160–1165.
26. Cammerer U, Dietrich W, Rampf T, Braun SL, Richter JA (2003) The predictive value of modified computerized thromboelastography and platelet function analysis for postoperative blood loss in routine cardiac surgery. *Anesth Analg* 96: 51–57.
27. Preisman S, Kogan A, Itzkovsky K, Leikin G, Raanani E (2010) Modified thromboelastography evaluation of platelet dysfunction in patients undergoing coronary artery surgery. *Eur J Cardiothorac Surg* 37: 1367–1374.
28. Ballotta A, Saleh HZ, El Baghdady HW, Gomaa M, Belloli F, et al. (2007) Comparison of early platelet activation in patients undergoing on-pump versus off-pump coronary artery bypass surgery. *J Thorac Cardiovasc Surg* 134: 132–138.
29. Basani RB, Richberg M, Poncz M (1999) Molecular biological identification and characterization of inherited platelet receptor disorders. *Methods Mol Med* 31: 313–336.
30. Kashuk JL, Moore EE, Sawyer M, Le T, Johnson J, et al. (2010) Postinjury coagulopathy management: goal directed resuscitation via POC thromboelastography. *Ann Surg* 251: 604–614.
31. Davis PK, Musunuru H, Walsh M, Cassady R, Yount R, et al. (2012) Platelet dysfunction is an early marker for traumatic brain injury-induced coagulopathy. *Neurocrit Care* 2012 Jul 31 [Epub ahead of print].
32. Holcomb JB, Mineci KM, Scerbo ML, Radwan ZA, Wade CE, et al. (2012) Admission rapid thromboelastography can replace conventional coagulation tests in the emergency department: experience with 1974 consecutive trauma patients. *Ann Surg* 256: 476–486.
33. Johansson PI (2012) Coagulation monitoring of the bleeding traumatized patient. *Current opinion in anaesthesiology* 25: 235–241.
34. Wohlaue MV, Moore EE, Thomas S, Sauaia A, Evans E, et al. (2012) Early platelet dysfunction: an unrecognized role in the acute coagulopathy of trauma. *J Am Coll Surg* 214: 739–746.
35. Walsh M, Thomas SG, Howard JC, Evans E, Guyer K, et al. (2011) Blood component therapy in trauma guided with the utilization of the perfusionist and thromboelastography. *J Extra Corp Tech* 43: 162–167.
36. Ikeda Y, Handa M, Kawano K, Kamata T, Murata M, et al. (1991) The role of von Willebrand factor and fibrinogen in platelet aggregation under varying shear stress. *J Clin Invest* 87: 1234–1240.
37. Cheng H, Yan R, Li S, Yuan Y, Liu J, et al. (2009) Shear-induced interaction of platelets with von Willebrand factor results in glycoprotein Ibalpha shedding. *Am J Physiol* 297: H2128–H2135.